

## Hydrogen Pentagraphenelike Structure Stabilized by Hafnium: A High-Temperature Conventional Superconductor

Hui Xie,<sup>1</sup> Yansun Yao,<sup>2</sup> Xiaolei Feng,<sup>3,4</sup> Defang Duan,<sup>1,5,\*</sup> Hao Song,<sup>1</sup> Zihan Zhang,<sup>1</sup> Shuqing Jiang,<sup>6,1</sup>  
Simon A. T. Redfern,<sup>7,3</sup> Vladimir Z. Kresin,<sup>8</sup> Chris J. Pickard,<sup>5,9,†</sup> and Tian Cui<sup>10,1,‡</sup>

<sup>1</sup>State Key Laboratory of Superhard Materials, College of Physics, Jilin University, Changchun 130012, China

<sup>2</sup>Department of Physics and Engineering Physics, University of Saskatchewan, Saskatoon, Saskatchewan S7N 5E2, Canada

<sup>3</sup>Center for High Pressure Science and Technology Advanced Research, Beijing 100094, China

<sup>4</sup>Department of Earth Science, University of Cambridge, Downing Site, Cambridge CB2 3EQ, United Kingdom

<sup>5</sup>Department of Materials Science & Metallurgy, University of Cambridge,  
27 Charles Babbage Road, Cambridge CB3 0FS, United Kingdom

<sup>6</sup>Synergetic Extreme Condition User Facility, College of Physics, Jilin University, Changchun, Jilin 130012, China

<sup>7</sup>Asian School of the Environment, Nanyang Technological University, Singapore 639798

<sup>8</sup>Lawrence Berkeley Laboratory, University of California at Berkeley, Berkeley, California 94720, USA

<sup>9</sup>Advanced Institute for Materials Research, Tohoku University, 2-1-1 Katahira, Aoba, Sendai 980-8577, Japan

<sup>10</sup>Institute of High Pressure Physics, School of Physical Science and Technology, Ningbo University, Ningbo 315211, China



(Received 4 March 2020; revised 7 July 2020; accepted 21 September 2020; published 16 November 2020)

The recent discovery of H<sub>3</sub>S and LaH<sub>10</sub> superconductors with record high superconducting transition temperatures  $T_c$  at high pressure has fueled the search for room-temperature superconductivity in the compressed superhydrides. Here we introduce a new class of high  $T_c$  hydrides with a novel structure and unusual properties. We predict the existence of an unprecedented hexagonal HfH<sub>10</sub>, with remarkably high value of  $T_c$  (around 213–234 K) at 250 GPa. As concerns the novel structure, the H ions in HfH<sub>10</sub> are arranged in clusters to form a planar “pentagraphenelike” sublattice. The layered arrangement of these planar units is entirely different from the covalent sixfold cubic structure in H<sub>3</sub>S and clathratelike structure in LaH<sub>10</sub>. The Hf atom acts as a precompressor and electron donor to the hydrogen sublattice. This pentagraphenelike H<sub>10</sub> structure is also found in ZrH<sub>10</sub>, ScH<sub>10</sub>, and LuH<sub>10</sub> at high pressure, each material showing a high  $T_c$  ranging from 134 to 220 K. Our study of dense superhydrides with pentagraphenelike layered structures opens the door to the exploration of a new class of high  $T_c$  superconductors.

DOI: 10.1103/PhysRevLett.125.217001

The development of room temperature superconductors is the ultimate goal for superconductivity research. The Bardeen-Cooper-Schrieffer theory suggests that metallic hydrogen is likely to be a good candidate for attaining high-temperature superconductivity, due to its high Debye temperature and strong electron-phonon coupling [1,2]. Conceptually, metallization can be achieved in pure hydrogen by dissociating the H<sub>2</sub> molecules under extreme conditions. Evidence for molecular dissociation has been found in high-pressure phases of solid hydrogen, where the vibron frequency decreases rapidly with increasing pressure [3], indicating the weakening of the intramolecular bonding. However, although there have been extensive attempts to synthesize metallic hydrogen [4,5], there is a lack of consensus on reported “successes,” and superconductivity has not been measured in any of the reported phases.

In the face of tremendous difficulties in synthesizing pure metallic hydrogen, many investigators have suggested that metallization can be achieved by “precompressing” hydrogen species in simple hydrides [6]. Highly compressed hydrogen-dominant hydrides are predicted to be

able to attain a metallic state and may, therefore, exhibit high  $T_c$  superconductivity. Recently, the search for high- $T_c$  superconductivity has been expanded from the known [7–9] to hitherto unknown hydrides, through high-pressure synthesis following theoretical predictions [10–23]. Remarkably, two of the predicted hydrides, H<sub>3</sub>S [11–13] and LaH<sub>10</sub> [17–19], have been successfully synthesized recently and exhibit record high  $T_c$  above 200 K. H<sub>3</sub>S has a bcc lattice of S with H atoms located halfway between the S atoms, exhibiting three-dimensional covalent metallic characteristics. LaH<sub>10</sub> has a three-dimensional clathratelike structure of H with La atoms filling the clathrate cavities, which has been described as an extended metallic hydrogen host structure stabilized by the guest electron donor (La).

By analyzing the superconducting properties of a large number of hydrides, we have summarized four criteria for finding high  $T_c$  superconductors in highly compressed hydrides (Figs. S1 and S2 [24]): (i) high symmetry crystal structure, (ii) absence of H<sub>2</sub>-like molecular units, (iii) a large H contribution to the total electronic density of states (DOS) at the Fermi level, and (iv) strong coupling of

electrons on the Fermi surface with high frequency phonons. The search for high- $T_c$  materials has been focused on two families of binary hydrides (see Table S1 [24]), covalent sixfold cubic structure [10–14] found in  $H_3S$  and  $H_3Se$ , and clathrate structure [15–22] found in rare earth hydrides  $REH_{10}$ ,  $REH_9$ , and  $REH_6$ . These two high- $T_c$  families satisfy the four criteria, with a common feature that they both adopt three-dimensional sublattices of hydrogen. On the other hand, pure solid hydrogen features pronounced layerlike characters. One example is the phase IV of hydrogen that consists of strongly bonded  $H_2$  molecules and weakly bonded graphenelike sheets [56–58]. This structure is considered as an important intermediate between the molecular (insulating) and atomic (metallic) crystalline phases of hydrogen. Many hydrides have been predicted to have a layered structure, but their  $T_c$  are not very high, e.g.,  $FeH_5$  [59],  $TeH_4$  [60], and  $KH_6$  [48], etc. One can raise a question: is there a layered structure of hydrogen-rich materials at high pressure that can achieve high  $T_c$ ? This question leads to the search for new physics and, more specifically, new structures and new concepts in this exciting field.

We introduce here a new class of superhydrides with novel structure and a number of unusual properties. We performed an extensive structure searching at high-pressure using AIRSS, USPEX, and CALYPSO codes [49–51] and indeed discovered a layered high- $T_c$  hafnium decahydride.

In  $HfH_{10}$ , the H atoms form planar clusters of three  $H_5$  pentagons, analogous to penta-graphene, while Hf atoms are intercalated between the clusters on the same plane. A new class of superhydrides,  $MH_{10}$  ( $M = Zr, Sc,$  and  $Lu$ ), which are isostructural to  $HfH_{10}$ , have also been predicted to possess high  $T_c$ .

Our main structure searching results for Hf-H system at high pressure are depicted in the convex hull diagrams of Figs. 1(a) and S3 in the Supplemental Material [24]. Considering the non-negligible quantum effects associated with hydrogen, the zero-point energy (ZPE) was included in the calculation of the formation enthalpies of predicted Hf-H compounds. We analyzed the stability of these compounds with respect to the elemental hafnium and hydrogen. As shown in Fig. 1(a), these searches revealed four stable stoichiometries at various pressures, e.g.,  $HfH$ ,  $HfH_3$ ,  $HfH_4$ , and  $HfH_{14}$ , in addition to the previously known  $HfH_2$  and  $Hf_4H_{15}$  [52,61]. Moreover,  $HfH_6$  and  $HfH_{10}$  are close to the convex hull ( $\sim 1$ – $2$  meV) at 300 GPa. A minor energy difference of this order already approaches the resolution of density functional theory calculation. For high-pressure synthesis, which usually involves high temperatures, the experimentally realized materials are often metastable phases [62]. The recently discovered high- $T_c$  superconducting  $LaH_{10}$  [18,19], for example, is a metastable compound lying above the convex hull that was previously predicted by Peng *et al.* [16].

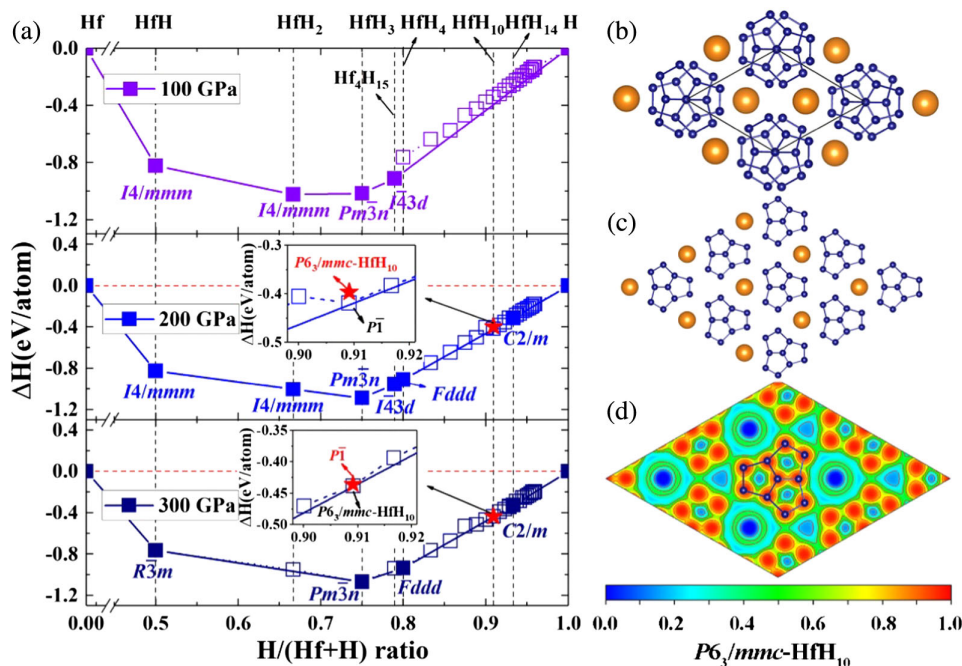


FIG. 1. (a) Formation enthalpies of predicted  $HfH_x$  ( $x = 1$ – $24$ ), including ZPEs with respect to decomposition into Hf and H under pressure. The  $Im\bar{3}m$  structure for hafnium [63], the  $P6_3/mc$ ,  $C2/c$ , and  $Cmca$ -12 structures for hydrogen [57] were adopted. Open symbols represent unstable configurations with respect to mixing lines on the convex hull, while solid symbols on the convex hull represent stable configurations. The red star near the convex hull represents the  $HfH_{10}$  phase with higher enthalpy. (b) The crystal structure of layered  $P6_3/mmc$  in  $HfH_{10}$ , where the layers are stacked in an ABAB fashion. (c) A layer of the  $P6_3/mmc$  structure. (d) ELF on the (001) plane. Golden (large) and small (blue) spheres represent Hf and H atoms, respectively.

For  $\text{HfH}_{10}$ , there are two energetically competitive structures, adopting  $P6_3/mmc$  and  $P\bar{1}$  symmetries (Tables S2 and S3 [24]). The  $P\bar{1}$  structure consists of diatomic hydrogen pairs similar to  $\text{H}_2$  molecules (Fig. S4 [24]), and this violates criteria (i) and (ii) for attaining high  $T_c$ . Intriguingly, the  $P6_3/mmc$  is a layered structure in which the Hf and H atoms are situated on the same plane [Figs. 1(b) and 1(c)]. The Hf atoms form a hexagonal sublattice interspersed by H atoms in unique  $\text{H}_5$  pentagons akin to the geometry of pentagraphene: three pentagons are fused by edge-sharing to form a  $\text{H}_{10}$  unit [Fig. 1(c)]. In the proceeding discussion, the superhydride  $P6_3/mmc\text{-HfH}_{10}$  is the main focus because it satisfies both criteria (i) high crystal symmetry and (ii) absence of  $\text{H}_2$  molecular unit.

We examine the chemical bonding of layered  $\text{HfH}_{10}$  by analyzing electron localization function (ELF), crystal orbital Hamiltonian population (COHP) and Bader charges. As shown in Figs. 1(d) and the Supplemental Material S5 [24], there is no charge localization between Hf and H, indicating that the Hf-H bonding is purely ionic. The ELF values for the  $\text{H}_{10}$  unit range between 0.6–0.8, showing the evidence for H-H covalent bonding. As depicted in Fig. S6 [24], the calculated COHP shows that most of the states below the Fermi level correspond to H-H bonding, consistent to H-H covalent bonds within the  $\text{H}_{10}$  unit. Furthermore, Bader charge analysis reveals that the planar  $\text{H}_{10}$  unit accepts an amount of charge, e.g.,  $\sim 0.13 e^-$  per H atom, from nearby Hf atoms, which results in longer H-H distances compared to that in free  $\text{H}_2$  molecule [64]. The additional electrons reside in the H-H antibonding orbital ( $\sigma^*$ ) and therefore weaken the H-H bonding, thus increasing the H-projected density of states (H-PDOS) at the Fermi level ( $\epsilon_f$ ).

To further explore this new form of hydrogen, we compared the H-H distances in  $\text{HfH}_{10}$  with those in  $\text{LaH}_{10}$  [17], atomic H [2], and the layered phase IV of H ( $Pc\text{-}48$ ) [56] structures. As shown in Fig. S7 [24], the longest nearest-neighbor H-H distance ( $d_{\text{H1-H2}}$ ) in  $\text{HfH}_{10}$  is close to the shortest H-H distance in  $\text{LaH}_{10}$  at the same pressure. The distance between H1 and H1 (second nearest neighbor) atoms approaches that of the atomic structure of hydrogen near 200 GPa. As the pressure increases, the shortest H-H bond length ( $d_{\text{H2-H3}}$ ) gets progressively closer to the H-H distances of  $Pc\text{-}48$  H ( $d_2$ ). Therefore, this pentagraphenelike hydrogen sublattice lies somewhere between atomic and layered hydrogen.

The discovery of apparently stable or metastable structures of  $\text{HfH}_{10}$  prompt us to further study the Zr-H system at 300 GPa (see Fig. S8 [24]). As it might be anticipated,  $\text{ZrH}_{10}$  adopts the same two competitive structures  $P\bar{1}$  and  $P6_3/mmc$  as  $\text{HfH}_{10}$ . According to the criterion (iii) for high  $T_c$  superconductivity, a large contribution by hydrogen to the total electronic DOS at the Fermi level is a critical factor for the development of exceptional superconducting properties. To this end, the projected electronic DOS of

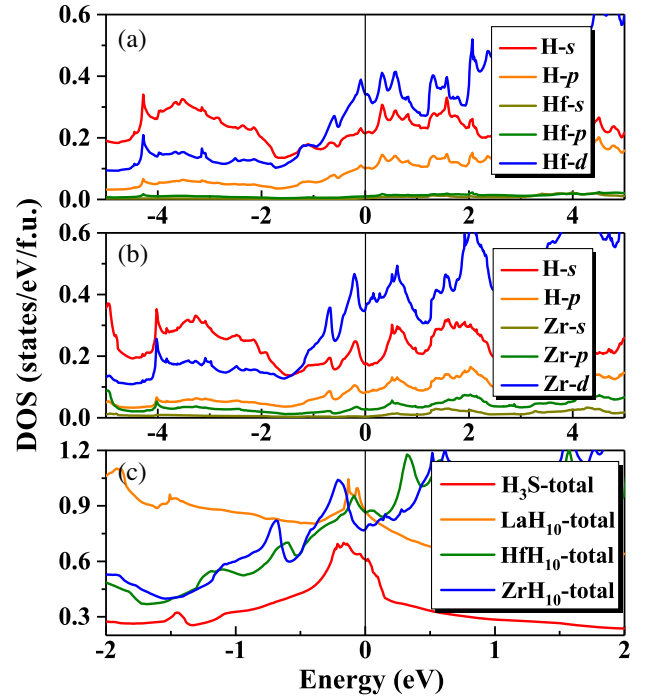


FIG. 2. Projected electronic DOS of (a)  $P6_3/mmc\text{-HfH}_{10}$  and (b)  $P6_3/mmc\text{-ZrH}_{10}$  at 300 GPa. (c) Total electronic DOS of  $\text{H}_3\text{S}$ ,  $\text{LaH}_{10}$ ,  $\text{HfH}_{10}$ , and  $\text{ZrH}_{10}$  around the van Hove singularities at 300 GPa.

$P6_3/mmc$  in  $\text{HfH}_{10}$  and  $\text{ZrH}_{10}$  were calculated [Fig. 2]. One can see that both phases are metallic with a large total electronic DOS and significant hydrogen contribution to the electronic DOS at the Fermi level. Remarkably, the electronic DOS exhibits van Hove singularities near the Fermi level, indicating a large electron-phonon coupling (EPC) strength bound up with hydrogen phonon modes. The total DOS of  $\text{H}_3\text{S}$ ,  $\text{LaH}_{10}$ ,  $\text{HfH}_{10}$ , and  $\text{ZrH}_{10}$  at 300 GPa are compared in Fig. 2(c). It is shown that  $\text{HfH}_{10}$  and  $\text{LaH}_{10}$  have a comparable electronic DOS at the Fermi level, and these are notably larger than those of  $\text{ZrH}_{10}$  and  $\text{H}_3\text{S}$ .

To examine the superconductivity in the layered pentagraphenelike structure, we calculate the average phonon frequency and EPC as shown in Table S5. For  $\text{HfH}_{10}$ , our EPC calculation yields a large  $\lambda$  of 2.16 at 300 GPa which is benefited from large H-PDOS and high frequency vibrations (above 10 THz) due to hydrogen which contribute 70% to the value of  $\lambda$  [Fig. 3(a)]. It is obvious that the large  $\lambda$  satisfies the last criterion (iv). Since  $\lambda$  is larger than 1.5, we calculated  $T_c$  using three approaches: Allen-Dynes modified McMillan equation (A–D) (Eq. S12 [24]) [53], Matsubara-type linearized Eliashberg equation (LE) [54], and Gor’kov-Kresin equation (G-K) [55], all of which were designed to estimate the  $T_c$  for materials with strong electron-phonon coupling. The results show that  $\text{HfH}_{10}$  is an extraordinary superconductor with a  $T_c$  of 151–166 K (A-D), 214–228 K (LE), and 197–220 K (G-K) using

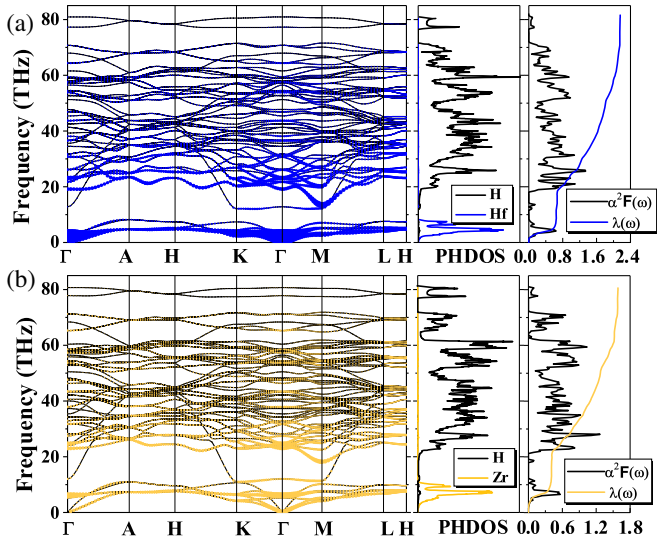


FIG. 3. Phonon dispersion curves (left), density of states (middle), and Eliashberg spectral function  $\alpha^2 F(\omega)$  together with the electron-phonon integral  $\lambda(\omega)$  (right) of (a) HfH<sub>10</sub> and (b) ZrH<sub>10</sub> at 300 GPa. The size of the solid dot on phonon spectra signifies the contribution to electron-phonon coupling.

$\mu^* = 0.1$ – $0.13$  at 300 GPa. To narrow down the range of  $T_c$ , we calculated the  $T_c$  of H<sub>3</sub>S and LaH<sub>10</sub> at 200 GPa and compared them to the experimental values to obtain appropriate parameters for this family of materials. As presented in Fig. S9 [24], the calculated  $T_c$  with  $\mu^* = 0.13$  using G-K and LE equations are close to the experimental values, while those estimated by A-D equation are much lower. In the following, we will estimate the  $T_c$ 's using the G-K equation. With the pressure decreased to 250 GPa,  $\lambda$  and  $T_c$  for HfH<sub>10</sub> increase to 2.77 and 213–234 K with  $\mu^* = 0.1$ – $0.13$ , respectively; these values are higher than those for H<sub>3</sub>S. For ZrH<sub>10</sub>, a large EPC parameter  $\lambda$  of 1.59 is calculated at 300 GPa, of which 74% is due to contributions by H atoms [Fig. 3(b)]. A high  $T_c$  of 194–218 K is therefore estimated for ZrH<sub>10</sub>. At 250 GPa,  $T_c$  increases to 199–220 K with a stronger  $\lambda$  of 1.77. We also calculated the electronic DOS and  $T_c$  of  $P\bar{1}$ -HfH<sub>10</sub> at 200 GPa (see Fig. S10 and Table S7 of Ref. [24]). It is found that, as expected, the existence of H<sub>2</sub> units reduce the electronic DOS at the Fermi level, and a low EPC parameter of 0.72, thereby limiting its superconductivity with  $T_c$  of 28.9–37.4 K ( $\mu^* = 0.1$ – $0.13$ ). Therefore, the four criteria for superconductivity provide important guidance in the search for high  $T_c$  superconductors in compressed superhydrides. Intriguingly, it is noted that high- $T_c$  hydrides HfH<sub>10</sub>, ZrH<sub>10</sub>, LaH<sub>10</sub>, or ternary Li<sub>2</sub>MgH<sub>16</sub> [65] with strong EPC are off the convex hull, suggesting that maybe one can search high  $T_c$  superconductors in compounds that are in the proximity of stability.

To further understand the superconductivity of the clathratelike and pentagraphenelike decahydrides, we compared the calculated  $T_c$ 's and essential parameters for

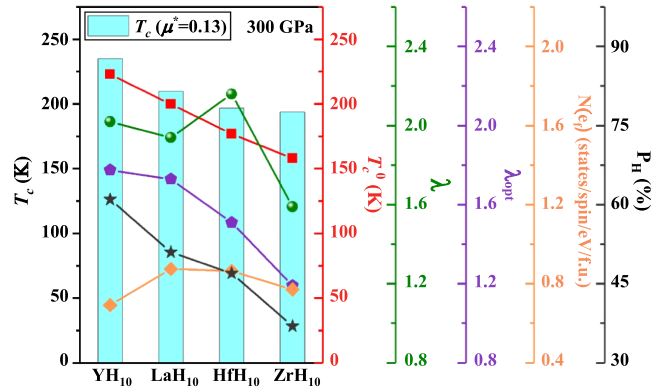


FIG. 4. Calculated superconducting parameters for YH<sub>10</sub>, LaH<sub>10</sub>, HfH<sub>10</sub>, and ZrH<sub>10</sub> at 300 GPa. The obtained  $T_c$  using G-K equation with  $\mu^* = 0.13$  ( $T_c$ ), the critical temperature caused by the interaction of electrons with optical phonons ( $T_c^0$ ), EPC parameter ( $\lambda$ ), strength of the interaction of electrons with optical phonons ( $\lambda_{opt}$ ), electronic DOS at the Fermi level  $N(\epsilon_f)$ , and the contribution of H atoms DOS to the total DOS at the Fermi energy ( $P_H$ ).

YH<sub>10</sub>, LaH<sub>10</sub>, HfH<sub>10</sub> and ZrH<sub>10</sub> at 300 GPa, illustrated in Fig. 4. We find that  $T_c$  decreases in the order of YH<sub>10</sub> > LaH<sub>10</sub> > HfH<sub>10</sub> > ZrH<sub>10</sub>, consistent with the decreasing trend of “optical” superconducting transition temperature caused by the interaction of electrons with optical phonons ( $T_c^0$ ), the contribution of H-PDOS to the total DOS at the Fermi level ( $P_H$ ) and “optical” electron-phonon coupling ( $\lambda_{opt}$ ). Thus, the high  $T_c$  in these hydrides is mainly attributed to the interaction of electrons with optical phonons and high DOS at the Fermi level associated with H atoms, in agreement with both superconducting criteria (iii) and (iv).

The fact that pentagraphenelike HfH<sub>10</sub> and ZrH<sub>10</sub> have very high  $T_c$  naturally raises the question: can any other hydrides adopt the same structure and display high  $T_c$  as well? The elements of Hf and Zr have three features in common: similar Pauling electronegativity ( $\sim 1.3$ ), similar atomic radius ( $\sim 1.6$  Å), and  $d$  states in valence subshells. After searching the periodic table of elements, we found that Mg, Sc, Lu, and Th have some similar properties. Phonon dispersion relations were calculated to test the stability of the corresponding decahydrides of these metals. The calculations did confirm that both ScH<sub>10</sub> and LuH<sub>10</sub> are dynamically stable, while MgH<sub>10</sub> and ThH<sub>10</sub> are not. For MgH<sub>10</sub> (Fig. S11 [24]) its dynamic instability could be due to the absence of  $d$  electrons in Mg and insufficient number of electrons transferred to H. For ThH<sub>10</sub> (Fig. S11 [24]), the large atomic radius of Th (1.8 Å) may be responsible for its dynamic instability. We note that the  $P6_3/mmc$  structure was first predicted by Peng *et al.* [16] for ScH<sub>10</sub>. However, this work is focused on the structure side, with little discussion on properties. Later, a  $Cmcm$  structure in ScH<sub>10</sub> was predicted [66]. We find that these phases are

competitive (Fig. S12 [24]). The EPC calculation for the  $P6_3/mmc$ -ScH<sub>10</sub> yields a  $\lambda$  of 1.16 and  $T_c$  ranging 134–158 K at 250 GPa (Figs. S13–S14 [24]). For Lu-H system, we perform extensive structure searching and find that LuH<sub>10</sub> with  $P6_3/mmc$  phase is stable at 300 GPa (Fig. S15 [24]). Phonon calculation shows that it is dynamically stable down to at least 200 GPa (Fig. S18 [24]). At 200 GPa, LuH<sub>10</sub> is found to be a good superconductor with a relatively high  $T_c$  of 134–152 K, comparable with to most other lanthanide hydrides. Although the emergence of  $5d$  electron in Lu suppresses the contribution of  $4f$  electrons and improves the contribution of hydrogen atoms at the Fermi level (Fig. S19 [24]), the relatively low total DOS at the Fermi level limits to some extent its superconductivity.

All of our calculations were carried out using the harmonic approximation. It is reported that in many hydrides anharmonicity tends to lower phase transition pressure and eliminate the pseudo dynamic instabilities [67,68]. The anharmonic effects may cause the dynamic stabilities of MgH<sub>10</sub> and ThH<sub>10</sub>, and stabilize HfH<sub>10</sub> and ZrH<sub>10</sub> at lower pressures, the analysis of which will be carried out elsewhere.

Since the substitution of deuterium for hydrogen (H  $\rightarrow$  D) affects the optical modes only, whereas the value of  $T_c$  is affected by both acoustic and optical modes, the value of the isotope coefficient and its closeness to the  $\alpha_{\max} = 0.5$  reflect the relative impact of the high frequency optical modes on  $T_c$  and the interplay of the optical and acoustic modes. It is worth mentioning that the value of  $T_c$  will be reduced upon H  $\rightarrow$  D substitution, since the high frequency hydrogen modes determine the value of the critical temperature in high- $T_c$  hydrides. Thus, the isotope coefficient ( $\alpha$ ) was calculated to estimate the  $T_c$  of MD<sub>10</sub> ( $T_c^D$ ). As shown in Table S5, the coefficients are 0.42–0.43 for HfH<sub>10</sub> at 250 GPa, 0.38–0.39 for ZrH<sub>10</sub> at 250 GPa, 0.37–0.38 for ScH<sub>10</sub> at 250 GPa, and 0.44–0.45 for LuH<sub>10</sub> at 200 GPa with  $\mu^* = 0.1$ –0.13, respectively. The  $\alpha$  values in these phases are relatively large, suggesting that the pairing, particularly in HfH<sub>10</sub> and LuH<sub>10</sub>, is dominated by the optical H modes, which yields the relatively low  $T_c^D$ . The  $T_c^D$  was described according to the equation of  $T_c/T_c^D = (M_H/M_D)^{-\alpha}$ , where  $T_c$  is obtained from the G-K equation. In our cases,  $T_c^D$  values are 159–174 K for HfD<sub>10</sub>, 153–168 K for ZrD<sub>10</sub>, 104–121 K for ScD<sub>10</sub>, and 99–111 K for LuD<sub>10</sub>, respectively, providing a reference for future experiments.

Our extensive first-principles structure searches have revealed the appearance of stable or metastable layered pentagraphenelike clustered H<sub>10</sub> structure in HfH<sub>10</sub>, ZrH<sub>10</sub>, ScH<sub>10</sub>, and LuH<sub>10</sub>. Electronegativity, atomic radius, and valence configuration of the metal element are all found to play critical roles in the stabilization of this novel hydrogen sublattice, and fine-tune the superconductivity of these materials. We want to pay a special attention to HfH<sub>10</sub>

which is predicted to be a high temperature superconductor with estimated  $T_c$  of 213–234 K at 250 GPa. It is the first example of the material, which contains two-dimensional structures in hydrogen-rich materials with high  $T_c$  above 200 K. It is also a hydride that has the highest  $T_c$  to date in the transition metal hydrides. The layered pentagraphene-like H<sub>10</sub> structure is a structural model for superconducting hydrides with  $T_c$  higher than 200 K, which is drastically different from the covalent bonded H structure in H<sub>3</sub>S and clathrate H structure in LaH<sub>10</sub>. One can state that at present there are three different model structures for high  $T_c$  hydrides. The new structure model described here further establish four criteria for high  $T_c$  superconductivity in hydrogen-rich materials proposed in this paper. The emergence of layered pentagraphenelike clustered H<sub>10</sub> structure is quite significant, which will stimulate further study of the hydrogen-based family of new superconducting materials and certainly help to develop this promising field. The formulated four criteria for high- $T_c$  superconductivity provide guidance for searching room-temperature superconductors in ternary or quaternary hydrogen-rich materials in the future, which have not been well explored to date.

We thank Professor Yanming Ma and Dr. Dmitrii V. Semenov for many interesting and stimulating discussions. This work was supported by the National Key R&D Program of China (No. 2018YFA0305900), National Natural Science Foundation of China (No. 51632002, No. 11674122, and No. 11974133), Program for Changjiang Scholars and Innovative Research Team in University (No. IRT\_15R23), and the Natural Sciences and Engineering Research Council of Canada (NSERC). C. J. P. acknowledges financial support from the Engineering and Physical Sciences Research Council (Grant EP/P022596/1) and a Royal Society Wolfson Research Merit award. X. F. acknowledges China Scholarship Council. X. F. acknowledges China Scholarship Council and Cambridge Trust. Parts of the calculations were performed in the High Performance Computing Center of Jilin University and TianHe-1(A) at the National Supercomputer Center in Tianjin.

\*Corresponding author.  
duandf@jlu.edu.cn

†Corresponding author.  
cjp20@cam.ac.uk

‡Corresponding author.  
cuitian@jlu.edu.cn

- [1] N. W. Ashcroft, *Phys. Rev. Lett.* **21**, 1748 (1968).
- [2] J. M. McMahon and D. M. Ceperley, *Phys. Rev. Lett.* **106**, 165302 (2011).
- [3] H.-k. Mao and R. J. Hemley, *Rev. Mod. Phys.* **66**, 671 (1994).
- [4] C. Ji, B. Li, W. Liu, J. S. Smith, A. Majumdar, W. Luo, R. Ahuja, J. Shu, J. Wang, S. Sinogeikin *et al.*, *Nature (London)* **573**, 558 (2019).

- [5] P. Loubeyre, F. Occelli, and P. Dumas, *Nature (London)* **577**, 631 (2020).
- [6] N. W. Ashcroft, *Phys. Rev. Lett.* **92**, 187002 (2004).
- [7] C. J. Pickard and R. J. Needs, *Phys. Rev. Lett.* **97**, 045504 (2006).
- [8] C. J. Pickard and R. J. Needs, *Phys. Rev. B* **76**, 144114 (2007).
- [9] M. I. Eremets, I. A. Trojan, S. A. Medvedev, J. S. Tse, and Y. Yao, *Science* **319**, 1506 (2008).
- [10] D. Duan, Y. Liu, F. Tian, D. Li, X. Huang, Z. Zhao, H. Yu, B. Liu, W. Tian, and T. Cui, *Sci. Rep.* **4**, 6968 (2015).
- [11] A. P. Drozdov, M. I. Eremets, I. A. Trojan, V. Ksenofontov, and S. I. Shylin, *Nature (London)* **525**, 73 (2015).
- [12] M. Einaga, M. Sakata, T. Ishikawa, K. Shimizu, M. I. Eremets, A. P. Drozdov, I. A. Trojan, N. Hirao, and Y. Ohishi, *Nat. Phys.* **12**, 835 (2016).
- [13] X. Huang, X. Wang, D. Duan, B. Sundqvist, X. Li, Y. Huang, H. Yu, F. Li, Q. Zhou, B. Liu *et al.*, *Natl. Sci. Rev.* **6**, 713 (2019).
- [14] S. Zhang, Y. Wang, J. Zhang, H. Liu, X. Zhong, H. F. Song, G. Yang, L. Zhang, and Y. Ma, *Sci. Rep.* **5**, 15433 (2015).
- [15] H. Liu, I. I. Naumov, R. Hoffmann, N. W. Ashcroft, and R. J. Hemley, *Proc. Natl. Acad. Sci. U.S.A.* **114**, 6990 (2017).
- [16] F. Peng, Y. Sun, C. J. Pickard, R. J. Needs, Q. Wu, and Y. Ma, *Phys. Rev. Lett.* **119**, 107001 (2017).
- [17] Z. M. Geballe, H. Liu, A. K. Mishra, M. Ahart, M. Somayazulu, Y. Meng, M. Baldini, and R. J. Hemley, *Angew. Chem. Int. Ed.* **57**, 688 (2018).
- [18] A. P. Drozdov, P. P. Kong, V. S. Minkov, S. P. Besedin, M. A. Kuzovnikov, S. Mozaffari, L. Balicas, F. F. Balakirev, D. E. Graf, V. B. Prakapenka *et al.*, *Nature (London)* **569**, 528 (2019).
- [19] M. Somayazulu, M. Ahart, A. K. Mishra, Z. M. Geballe, M. Baldini, Y. Meng, V. V. Struzhkin, and R. J. Hemley, *Phys. Rev. Lett.* **122**, 027001 (2019).
- [20] P. Kong, V. Minkov, M. Kuzovnikov, S. Besedin, A. Drozdov, S. Mozaffari, L. Balicas, F. Balakirev, V. Prakapenka, and E. Greenberg, [arXiv:1909.10482](https://arxiv.org/abs/1909.10482).
- [21] A. G. Kvashnin, D. V. Semenok, I. A. Kruglov, I. A. Wrona, and A. R. Oganov, *ACS Appl. Mater. Interfaces* **10**, 43809 (2018).
- [22] D. V. Semenok, A. G. Kvashnin, A. G. Ivanova, V. Svitlyk, V. Y. Fominski, A. V. Sadakov, O. A. Sobolevskiy, V. M. Pudalov, I. A. Trojan, and A. R. Oganov, *Mater. Today* **33**, 36 (2020).
- [23] H. Wang, J. S. Tse, K. Tanaka, T. Iitaka, and Y. Ma, *Proc. Natl. Acad. Sci. U.S.A.* **109**, 6463 (2012).
- [24] See Supplemental Material at <http://link.aps.org/supplemental/10.1103/PhysRevLett.125.217001> for computational details, equations for calculating  $T_c$  and related parameters, electronic structures, phonon dispersion curves, phase diagrams, and structural information of all predicted Hf-H and MH<sub>10</sub> compounds, which includes Refs. [10–11, 14–16, 18–23, 25–55].
- [25] M. D. Segall, J. D. L. Philip, M. J. Probert, C. J. Pickard, P. J. Hasnip, S. J. Clark, and M. C. Payne, *J. Phys. Condens. Matter* **14**, 2717 (2002).
- [26] G. Kresse and J. Furthmüller, *Comput. Mater. Sci.* **6**, 15 (1996).
- [27] J. P. Perdew, K. Burke, and M. Ernzerhof, *Phys. Rev. Lett.* **77**, 3865 (1996).
- [28] P. Blaha, K. Schwarz, P. Sorantin, and S. Trickey, *Comput. Phys. Commun.* **59**, 399 (1990).
- [29] F. Birch, *J. Appl. Phys.* **9**, 279 (1938).
- [30] A. D. Becke and K. E. Edgecombe, *J. Chem. Phys.* **92**, 5397 (1990).
- [31] R. Dronskowski and P. E. Bloechl, *J. Phys. Chem.* **97**, 8617 (1993).
- [32] G. Henkelman, A. Arnaldsson, and H. Jónsson, *Comput. Mater. Sci.* **36**, 354 (2006).
- [33] A. Togo, F. Oba, and I. Tanaka, *Phys. Rev. B* **78**, 134106 (2008).
- [34] J. P. Perdew, A. Ruzsinszky, G. I. Csonka, O. A. Vydrov, G. E. Scuseria, L. A. Constantin, X. Zhou, and K. Burke, *Phys. Rev. Lett.* **100**, 136406 (2008).
- [35] P. Giannozzi, S. Baroni, N. Bonini, M. Calandra, R. Car, C. Cavazzoni, D. Ceresoli, G. L. Chiarotti, M. Cococcioni, I. Dabo *et al.*, *J. Phys. Condens. Matter* **21**, 395502 (2009).
- [36] G. Eliashberg, *JETP* **11**, 696 (1960).
- [37] L. P. Gor'kov and V. Z. Kresin, *Sci. Rep.* **6**, 25608 (2016).
- [38] G. Bergmann and D. Rainer, *Z. Phys.* **263**, 59 (1973).
- [39] D. Rainer and G. Bergmann, *J. Low Temp. Phys.* **14**, 501 (1974).
- [40] P. B. Allen, Technical Report No. 7, TCM/4/1974 (1974).
- [41] X. Feng, J. Zhang, G. Gao, H. Liu, and H. Wang, *RSC Adv.* **5**, 59292 (2015).
- [42] Y. Li, J. Hao, H. Liu, J. S. Tse, Y. Wang, and Y. Ma, *Sci. Rep.* **5**, 9948 (2015).
- [43] D. V. Semenok, A. G. Kvashnin, I. A. Kruglov, and A. R. Oganov, *J. Phys. Chem. Lett.* **9**, 1920 (2018).
- [44] J. Hooper, B. Altintas, A. Shamp, and E. Zurek, *J. Phys. Chem. C* **117**, 2982 (2013).
- [45] D. C. Lonie, J. Hooper, B. Altintas, and E. Zurek, *Phys. Rev. B* **87**, 054107 (2013).
- [46] E. Zurek, R. Hoffmann, N. W. Ashcroft, A. R. Oganov, and A. O. Lyakhov, *Proc. Natl. Acad. Sci. U.S.A.* **106**, 17640 (2009).
- [47] W. L. McMillan, *Phys. Rev.* **167**, 331 (1968).
- [48] D. Zhou, X. Jin, X. Meng, G. Bao, Y. Ma, B. Liu, and T. Cui, *Phys. Rev. B* **86**, 014118 (2012).
- [49] C. J. Pickard and R. J. Needs, *J. Phys. Condens. Matter* **23**, 053201 (2011).
- [50] A. R. Oganov and C. W. Glass, *J. Chem. Phys.* **124**, 244704 (2006).
- [51] Y. Wang, J. Lv, L. Zhu, and Y. Ma, *Phys. Rev. B* **82**, 094116 (2010).
- [52] M. A. Kuzovnikov and M. Tkacz, *J. Phys. Chem. C* **123**, 30059 (2019).
- [53] P. B. Allen and R. C. Dynes, *Phys. Rev. B* **12**, 905 (1975).
- [54] I. A. Kruglov, D. V. Semenok, H. Song, R. Szcześniak, I. A. Wrona, R. Akashi, M. M. Davari Esfahani, D. Duan, T. Cui, and A. G. Kvashnin, and A. R. Oganov, *Phys. Rev. B* **101**, 024508 (2020).
- [55] L. P. Gor'kov and V. Z. Kresin, *Rev. Mod. Phys.* **90**, 011001 (2018).
- [56] C. J. Pickard, M. Martinez-Canales, and R. J. Needs, *Phys. Rev. B* **85**, 214114 (2012).
- [57] C. J. Pickard and R. J. Needs, *Nat. Phys.* **3**, 473 (2007).

- [58] R. T. Howie, C. L. Guillaume, T. Scheler, A. F. Goncharov, and E. Gregoryanz, *Phys. Rev. Lett.* **108**, 125501 (2012).
- [59] C. M. Pépin, G. Geneste, A. Dewaele, M. Mezouar, and P. Loubeyre, *Science* **357**, 382 (2017).
- [60] X. Zhong, H. Wang, J. Zhang, H. Liu, S. Zhang, H. F. Song, G. Yang, L. Zhang, and Y. Ma, *Phys. Rev. Lett.* **116**, 057002 (2016).
- [61] Y. Liu, X. Huang, D. Duan, F. Tian, H. Liu, D. Li, Z. Zhao, X. Sha, H. Yu, H. Zhang *et al.*, *Sci. Rep.* **5**, 11381 (2015).
- [62] Y. Wu, P. Lazic, G. Hautier, K. Persson, and G. Ceder, *Energy Environ. Sci.* **6**, 157 (2013).
- [63] H. Xia, G. Parthasarathy, H. Luo, Y. K. Vohra, and A. L. Ruoff, *Phys. Rev. B* **42**, 6736 (1990).
- [64] V. Labet, P. Gonzalez-Morelos, R. Hoffmann, and N. W. Ashcroft, *J. Chem. Phys.* **136**, 074501 (2012).
- [65] Y. Sun, J. Lv, Y. Xie, H. Liu, and Y. Ma, *Phys. Rev. Lett.* **123**, 097001 (2019).
- [66] X. Ye, N. Zarifi, E. Zurek, R. Hoffmann, and N. W. Ashcroft, *J. Phys. Chem. C* **122**, 6298 (2018).
- [67] I. Errea, M. Calandra, C. J. Pickard, J. Nelson, R. J. Needs, Y. Li, H. Liu, Y. Zhang, Y. Ma, and F. Mauri, *Phys. Rev. Lett.* **114**, 157004 (2015).
- [68] M. Borinaga, I. Errea, M. Calandra, F. Mauri, and A. Bergara, *Phys. Rev. B* **93**, 174308 (2016).